Available online at www.sciencedirect.com

ScienceDirect

Progress in Natural Science: Materials International 24 (2014) 226–231

Progress in Natural Science Materials International

www.elsevier.com/locate/pnsmi
www.sciencedirect.com

Original Research

Uniform fabrication of Ge nanocrystals embedded into SiO_2 film via neutron transmutation doping

Wei Liu[a], Tiecheng Lu[a,*], Qingyun Chen[b], Youwen Hu[a], Shaobo Dun[a], Issai Shlimak[c]

[a]Department of Physics and Key Laboratory for Radiation Physics and Technology of Ministry of Education, Sichuan University, Chengdu 610064, China
[b]School of National Defence and Technology, Southwest University of Science and Technology, Mianyang 621010, China
[c]Minerva Center and Jack and Pearl Resnick Institute of Advanced Technology, Department of Physics, Bar-Ilan University, Ramat-Gan 52900, Israel

Received 31 October 2013; accepted 12 February 2014
Available online 23 May 2014

Abstract

Nanocrystalline ^{74}Ge embedded SiO_2 films were prepared by employing ion implantation and neutron transmutation doping methods. Transmission electron microscopy, energy dispersive x-ray spectroscopy, and photoluminescence of the obtained samples were measured. The existence of As dopants transmuted from ^{74}Ge is significant to guarantee the uniformity and higher volume density of Ge nanocrystals by tuning the system's crystallinity and activating mass transfer process. It was observed that the photoluminescence intensity of Ge nanocrystals increased first then decreased with the increase of arsenic concentration. The optimized fluence of neutron transmutation doping was found to be 5.5×10^{17} cm^{-2} to achieve maximum photoluminescence emission in Ge embedded SiO_2 film. This work opens a route in the three-dimensional nanofabrication of uniform Ge nanocrystals.

Keywords: Ge nanocrystals; Ion implantation; Neutron transmutation doping; Photoluminescence property

1. Introduction

The visible light emission from group IV nanocrystals has aroused interest of worldwide scientists recently because of their potential application in Si-based optoelectronic devices [1,2]. Germanium nanocrystals (Ge-NCs) embedded into SiO_2 matrix have attracted increasing attention due to the property of visible detecting and near infrared photoluminescence (PL) and ability to maintain the injected charge during a sufficiently long time necessary for memory devices [3–5]. On the other hand, method of Ge-NCs fabrication which consists in Ge^+ ion implantation into the SiO_2 layer on the Si surface is fully compatible with the current microelectronic technology. This gives a possibility to develop novel optoelectronic devices using the vast fabrication capabilities of the modern Si-based semiconductor industry [6,7]. Moreover, the additional important advantage of Ge-NCs is the ability to withstand the strong damaging radiation which gives rise to developing devices that can operate under extreme conditions, such as the one existing in the outer space [8–10].

To realize the enhancement of light emission and electric transportation property, uniform shape and ordered size distribution of Ge-NCs are indispensable. To date, extensive efforts have been made to improve the uniformity of nanocrystals [11,12]. However, so far only two-dimensional periodic array uniform NCs have been obtained. Achieving uniform NCs under 3D confinement conditions remains one of the most daunting challenges. Neutron transmutation doping (NTD) is a technique which utilizes the nuclear reaction of thermal neutrons with the isotopes in a semiconductor material [13–15] and it has been reported that impurities are distributed homogeneously in a material by adapting NTD process [16–18]. Besides, extensive doping methods of both physics

*Corresponding author. Tel./fax: +86 2885412031.
E-mail address: lutiecheng@scu.edu.cn (T. Lu).
Peer review under responsibility of Chinese Materials Research Society.

Production and hosting by Elsevier

http://dx.doi.org/10.1016/j.pnsc.2014.04.005
1002-0071/

and chemistry combined with NTD technique give more room for tuning the size and uniformity of NCs in larger scale, thus providing the possibility to investigate the correlation among the structural, optical and electrical properties of these NCs, such as the photoluminescence and *C–V* characteristics.

In this paper, we report a systematic study on fabricating uniform Ge-NCs embedded SiO_2 films via successive procedures, including the ion-implantation and NTD-assisted doping of Ge-NCs. The influences of key factors including the implantation fluences, neutron irradiation fluence, as well as the second annealing on the uniformity and volume density of Ge-NCs have been investigated. The non-monotonic PL behavior with variation of As-doping concentration was also observed and the optimized NTD fluence for maximum photoluminescence emission has been given.

2. Material and methods

2.1. Ge nanocrystals preparation

The isotope nanocrystalline ^{74}Ge samples were prepared by isotopic ^{74}Ge-ion implantation, followed by thermal annealing. Ion implantation was performed in a LC-4 high-energy ion implanter in a 10^{-5} Torr vacuum atmosphere. Gas GeH_4 was ionized into Ge^+ and Ge^{2+} by arc discharging. Isotope $^{74}Ge^+$ ions accelerated to 150 keV were selected by magnetism analysis equipment (the mass resolution of magnet $m/\Delta m$=120), and implanted into amorphous SiO_2 film, which was thermally grown on a p-type (100) Si matrix. The fluences of $^{74}Ge^+$ ions from $1\times10^{16}\,cm^{-2}$ to $1\times10^{18}\,cm^{-2}$ were used for implantation. After implantation, samples were annealed at 800 °C for 0.5 h in a forming gas (10% H_2 and 90% Ar) atmosphere (labeled as undoped Ge-NCs). Neutron irradiation was performed in a nuclear reactor by laying the samples in the nuclear reactor, with integral thermal neutron fluences of $3\times10^{16}\,cm^{-2}$, $1\times10^{17}\,cm^{-2}$, $1\times10^{19}\,cm^{-2}$ and $1\times10^{20}\,cm^{-2}$. Donor impurity ^{75}As is transmuted from ^{74}Ge by NTD. Second annealing is performed at 800 °C in the same forming gas atmosphere for 0.5 h to eliminate any irradiation induced defect and to recrystallize the Ge-NCs.

2.2. Characterization

High-resolution, scanning transmission electron microscopy (TEM and STEM) as well as elements mapping images were obtained with JEOL 2010 FEG transmission electron microscope attached with energy dispersive x-ray spectroscopy (EDS). The PL spectra were measured on a Renishaw-1000 fluorescence spectrometer and excited by the 514.5 nm line of the Ar^+ laser at room temperature.

3. Results and discussion

Impact of different Ge-ion doses on the formation of Ge-NCs was studied first. Amorphous SiO_2 films thermally grown on a p-type [100] Si matrix were implanted with different Ge-ion doses via fluences of $1\times10^{16}\,cm^{-2}$, $1\times10^{17}\,cm^{-2}$, $5\times10^{17}\,cm^{-2}$, and $1\times10^{18}\,cm^{-2}$. The microscopy results are shown in Fig. 1. After the implantation with low fluence ($1\times10^{16}\,cm^{-2}$ or less), none of Ge nanoparticles were found in the outermost layer near the SiO_2 surface (since no stronger scattering contrast from Ge atoms was observed). As the Ge-ion fluence was increased to $1\times10^{17}\,cm^{-2}$, finite dark clusters formed in the ~50 nm thickness range of SiO_2 layer. On further increasing the fluence fivefold, Ge nanoparticles near the SiO_2 surface grew bigger and decreased deeply forward (Fig. 1c). When the implantation fluence increased up to $1\times10^{18}\,cm^{-2}$, the decreased gradient of particle size was weak and Ge-NCs were in the size range of 8–17 nm. The results above demonstrate an obvious growing manner coupled with the increase of implantation fluence, which is crucial to practically optimize the original size distribution of Ge-NCs. Herein, the sample implanted with fluence of $1\times10^{17}\,cm^{-2}$

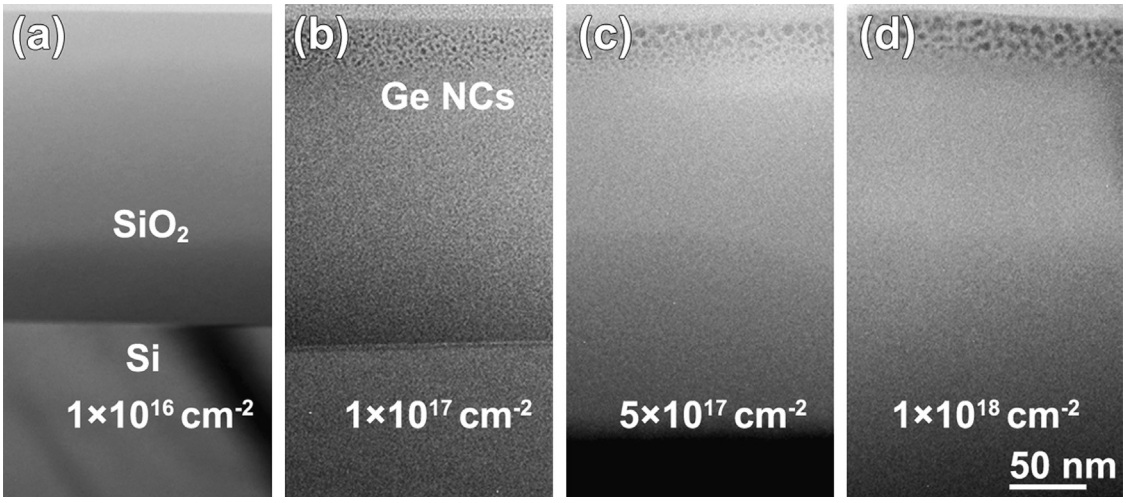

Fig. 1. Bright field STEM images of Ge-NCs after different Ge implantation fluences. The implantation fluences are $1\times10^{16}\,cm^{-2}$, $1\times10^{17}\,cm^{-2}$, $5\times10^{17}\,cm^{-2}$, and $1\times10^{18}\,cm^{-2}$ increasing from (a) to (d), respectively.

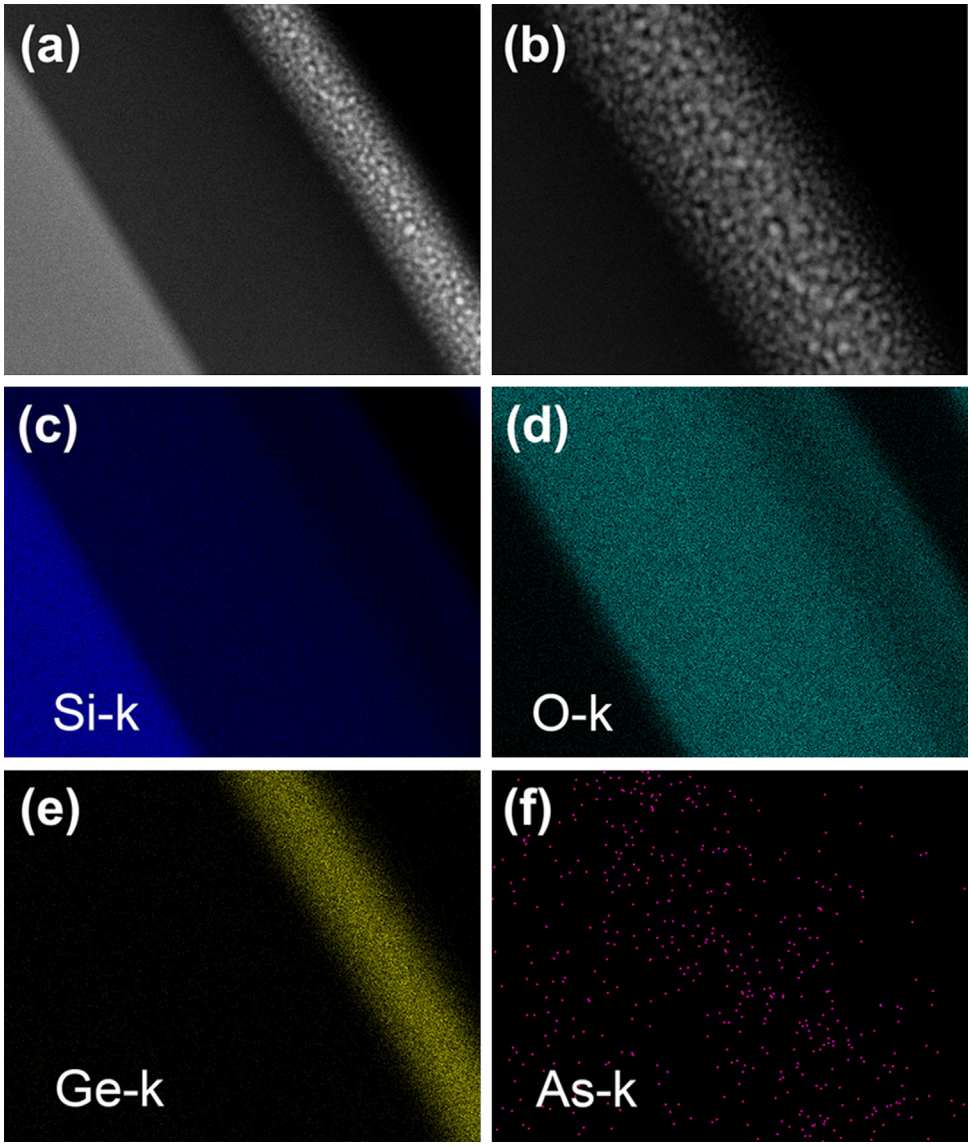

Fig. 2. Elements distribution of a typical doped Ge-NCs. (a, b) Low and high magnified DF-STEM images of the doped Ge-NCs; (c)–(f) EDS mapping images of Si, O, Ge, and As.

was selected for the following NTD treatment due to its uniformity and finite size of implanted Ge-NCs.

The doping of Ge-NCs sample was achieved through thermal neutron irradiation with different fluences. An STEM and EDS combined method was utilized to elucidate the elements' distribution of the $Ge/SiO_2/Si$ layered structure, as shown in Fig. 2. The dark-field STEM images (Fig. 2a and b) provide the atomic number (z^2)-dependence contrast distribution in the whole scanning area. Since the brightness is proportional to the mass density (thickness of the sample was considered uniform in such a small area), the contrast contributed from SiO_2, Si, and Ge should turn to be brighter in sequence. Further EDS mapping results confirm the above deduction (Fig. 2c–f). Signals' distribution from the k-edges of the corresponding elements coincides with the contrast distribution. It should be noted that the arsenic signal was rather weak due to its low concentration (less than 0.01%, which has exceeded the resolution limit of EDS); however, it still depicted the rough position of arsenic element, which is near the Ge layer. This could be evidence of the NTD effect showing the existence of arsenic element, which shows a good agreement with the XPS characterization performed in the former work. [8]

Fig. 3 shows the low magnified cross-section and high resolution TEM (HRTEM) images of the undoped Ge-NCs and heavily doped Ge-NCs samples (both samples are implanted by Ge ion dose of $1 \times 10^{17}\,cm^{-2}$). In Fig. 3(a), Ge-NCs particles well disperse in the zone with thickness of ~43 nm near the surface of SiO_2 film. The lattice fringes illustrated in the inset can be indexed to the (111) plane of face centered cubic (FCC) Ge nanocrystals. In Fig. 3(b), size and distribution conditions of doped nanocrystals exhibit a significant difference from the undoped one (Fig. 3a). The entire Ge component disperses into a much thicker layer (~54 nm) demonstrating a

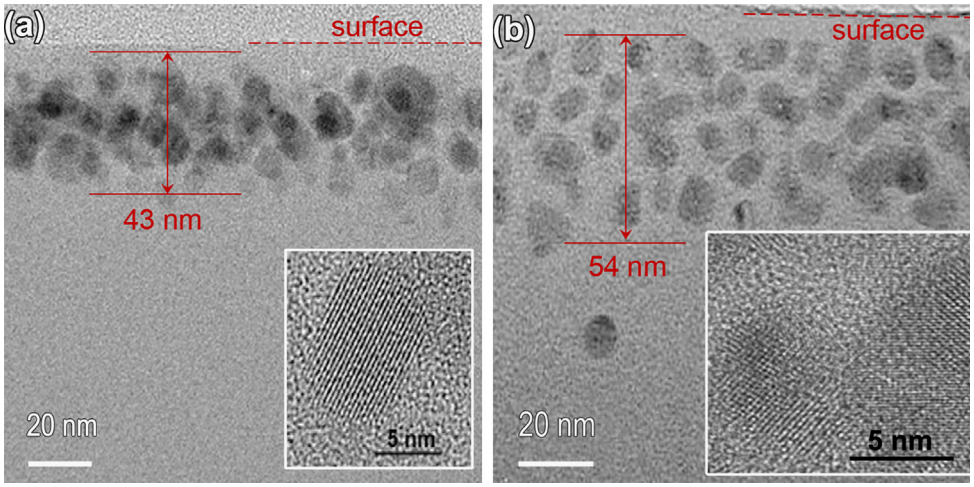

Fig. 3. TEM images of (a) undoped Ge-NCs and (b) heavily doped Ge-NCs (fluence of 1×10^{20} cm^{-2}) samples; the insets are their corresponding HRTEMs. The surfaces of SiO_2 layers are marked with red dashed line; the thickness of Ge-NCs layer is measured as well.

much uniform distribution of nanocrystals in 3D. According to the statistics analysis, the mean sizes are 10.2 nm for the undoped sample and 11.5 nm for the doped sample. The average size increases with introducing impurities in the sample, which could be ascribed to the lattice expansion resulted from the As atom doping. The size distribution of doped sample (7–17 nm) is narrower than the undoped one (4–19 nm). The above evidence proves the significant promotion of size and distribution of Ge-NCs induced by NTD.

The annealing effect on the doped Ge-NCs was also investigated so as to have an in-depth insight into the influence of NTD processing on the uniformity and crystallinity of Ge-NCs. As shown in Fig. 4, HRTEM images reveal that no obvious lattice fringes were found in the sample before annealing; the selected area diffraction pattern (inset in Fig. 4a) coming from the whole area manifests typical intensity distribution of an amorphous material. While in the sample which has undergone annealing treatment, there is an evident improvement on the crystallinity. The main resolved lattice fringes could be indexed to Ge(200) of FCC structure. An apparent diffraction ring (inset of Fig. 4b) could be identified to the polycrystalline FCC structure, implying random orientation distribution of the Ge-NCs in the annealed sample. The above microscopy results disclose the important role of annealing effect on the crystallinity promotion of Ge-NCs.

On the basis of *ab initio* calculation in our former work [8], the formation mechanism of uniform Ge-NCs can be interpreted as follows. For the undoped NCs, the local high-temperature nucleates Ge ions into Ge-NCs after Ge-ion implantation because the annealing procedure follows the minimum energy principle; the Gibbs free energy of a nanoparticle aggregated from ions is much lower than the energy sum of these ions. However, the non-simultaneous aggregation procedure must lead to the nonhomogeneous formation and thus to the nonuniformity of size distribution of Ge-NCs. While after the NTD treatment, the spatial uniform dispersion of irradiation ensures the 3D uniformity of As doping. The as-doped As atoms serve as nucleation sites and induce the recrystallization of Ge-NCs after the NTD irradiation, breaking the former NCs into amorphous ones. This recrystallization procedure was carried out in the second annealing after NTD, which produces Ge-NCs of high uniformity in 3D.

Since the NTD treatment promotes the uniformity of Ge-NCs in SiO_2 film, the irradiation fluence of NTD should have an impact on the optical properties of as-fabricated samples. The PL spectra of doped Ge-NCs with different impurity concentrations (different NTD fluences) are shown in Fig. 5(a). All of the spectra are normalized at their maximum intensities and scaling factors (a larger factor correspond to a smaller PL intensity). The PL intensity of doped nanocrystals increases then decreases with increasing thermal neutron fluence (shown in Fig. 5a curves a–e). The blueshift of visible luminescence band centered at 620 nm could be attributed to the quantum confinement effect [19–21]. Another broad luminescence emission band peak at 750 nm is independent of nanocrystals' size. It should originate from defect optical centers, not exciton luminescence. It is well known that there are two PL bands in a Ge implanted SiO_2 film; one is related to defects' luminescence in SiO_2 matrices (peaks at 680 nm) [22]; the other is attributed to $T_{\Pi}' \rightarrow S_0$ optical transitions in GeO color centers (peaks at 780 nm) [23]. In our opinion, the PL band at 750 nm is the complex luminescence of above two PL bands. Fig. 5(b) illustrates the thermal neutron fluence dependence of maximum exciton PL intensity (peaks around 600 nm). It indicates that the exciton PL emission intensity increases with the increasing of doping concentration and then decreases in heavily doped Ge-NCs sample. This non-monotonic photoluminescence behavior can be explained with two physical processes: the passivation of non-radiative centers (low arsenic concentration), and the reduction of radiative efficiency (high arsenic concentration) induced by auger-like recombination channel [24–26]. Such similar phenomena have been reported in the case of doping SiGe nanocrystals with P impurities

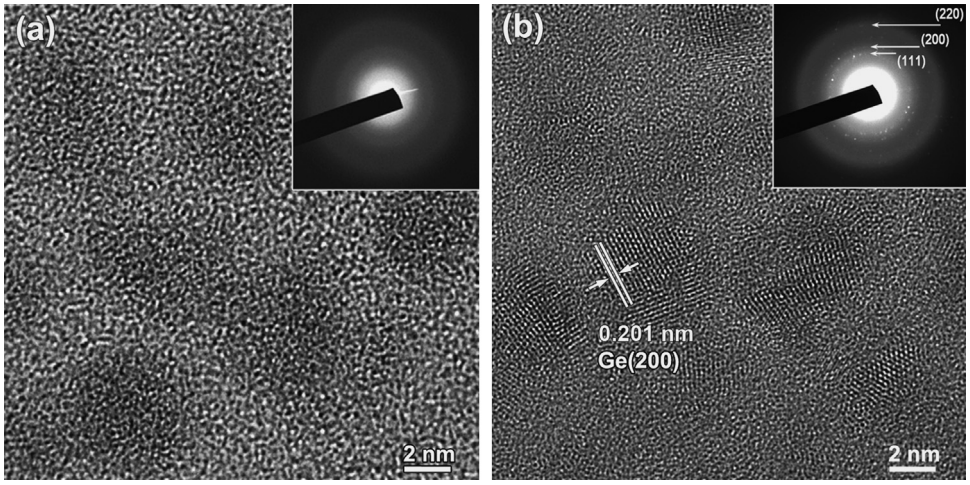

Fig. 4. TEM images the doped Ge-NCs before (a) and after (b) the second annealing; the insets are their corresponding selected area diffraction patterns.

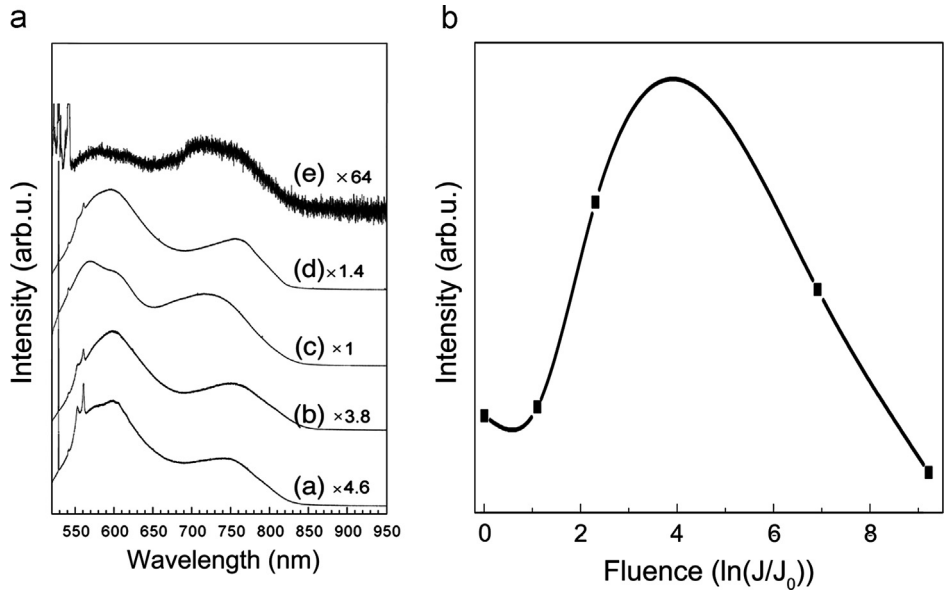

Fig. 5. PL properties of Ge-NCs irradiated with different NTD fluences: (a) PL spectra of Ge-NCs after second annealing; all the spectra are normalized at their maximum intensities and scaling factors are given: (a) undoped Ge-NCs; (b)–(e) Ge-NCs irradiated with thermal neutron fluence of $3\times10^{16}\,cm^{-2}$, $1\times10^{17}\,cm^{-2}$, $1\times10^{19}\,cm^{-2}$, and $1\times10^{20}\,cm^{-2}$, respectively; (b) thermal neutron fluence dependence of maximum exciton PL intensity, where J is the actual fluence, $J_0=1\times10^{16}\,cm^{-2}$, and leftmost data point corresponds to undoped Ge-NCs.

[27,28]. The fitted peak in Fig. 5(b) appears at a fluence of $\sim4\ln(J/J_0)$, which implies that the maximum intensity PL emission could be achieved using Ge-NCs embedded SiO_2 film via NTD irradiation with fluence of $\sim5.5\times10^{17}\,cm^{-2}$.

4. Conclusions

In this work, NTD method is adapted to prepare ^{74}Ge-NCs embedded SiO_2 film of high uniformity. Microscopy observation reveals that the As dopants transmuted from ^{74}Ge by NTD is of critical importance to form uniform and high volume density of Ge-NCs in space of 3D cooperated with thermal annealing. The competition between passivation of non-radiative centers and the radiative-efficiency reduction induced by free donor electrons drives the PL intensity of doped Ge-NCs to increase first and then decrease with increase of As dopant concentration. The optimized fluence of neutron transmutation doping is found to be $5.5\times10^{17}\,cm^{-2}$ to achieve maximum photoluminescence emission in Ge embedded SiO_2 film. This work opens a route in the three-dimensional nanofabrication of uniform Ge nanocrystals for the Si-based optoelectronic devices.

Acknowledgments

This work is supported by the National Natural Science Foundation of China (Grant no. 50872083, 51002098, 11304209 and 11145006), the Doctoral Program of Higher

Education (Grant no. 20090181120092) and Start Science Foundation of Sichuan University for Young Teachers (Grant no. 2012SCU11084).

References

[1] L. Pavesi, L. Dal Negro, C. Mazzoleni, G. Franzo, F. Priolo, Nature 408 (2000) 440–444.
[2] S. Godefroo, M. Hayne, M. Jivanescu, A. Stesmans, M. Zacharias, O. I. Lebedev, G. Van Tendeloo, V.V. Moshchalkov, Nat. Nanotechnol. 3 (2008) 174–178.
[3] K.D. Hirschman, L. Tsybeskov, S.P. Duttagupta, P.M. Fauchet, Nature 384 (1996) 338–341.
[4] H.Z. Song, X.M. Bao, Phys. Rev. B 55 (1997) 6988–6993.
[5] I.V. Antonova, V.I. Popov, S.A. Smagulova, J. Jedrzejewski, I. Balberg, J. Appl. Phys. 113 (2013) 084308.
[6] L.C. Gontard, J.R. Jinschek, H.Y. Ou, J. Verbeeck, R.E. Dunin-Borkowski, Appl. Phys. Lett. 100 (2012) 263113.
[7] C.J. Huang, J.Z. Yu, Q.M. Wang, Prog. Nat. Sci. 14 (2004) 388–395.
[8] Q. Chen, T. Lu, M. Xu, C. Meng, Y. Hu, K. Sun, I. Shlimak, Appl. Phys. Lett. 98 (2011) 073103.
[9] S.B. Dun, T.C. Lu, Y.W. Hu, Q. Hu, L.Q. Yu, Z. Li, N.K. Huang, S. B. Zhang, B. Tang, J.L. Dai, L. Resnick, I. Shlimak., J. Lumin. 128 (2008) 1363–1368.
[10] S. Levy, I. Shlimak, A. Chelly, Z. Zalevsky, T.C. Lu, Physica B 404 (2009) 5189–5191.
[11] X. Qian, J. Li, D. Wasserman, W.D. Goodhue, Appl. Phys. Lett. 93 (2008) 231907.
[12] T. Ujihara, Y. Yoshida, W.S. Lee, Y. Takeda, Appl. Phys. Lett. 89 (2006) 083110.
[13] Y.W. Hu, T.C. Lu, S.B. Dun, Q. Hu, N.K. Huang, S.B. Zhang, B. Tang, J.L. Dai, L. Resnick, I. Shlimak, S. Zhu, Q.M. Wei, L.M. Wang, Solid State Commun. 141 (2007) 514–518.
[14] S.B. Dun, T.C. Lu, Y.W. Hu, Q. Hu, C.F. You, N.K. Huang, Mater. Lett. 62 (2008) 3617–3619.
[15] Y.W. Hu, T.C. Lu, S.B. Dun, Q. Hu, C.F. You, Q.Y. Chen, N.K. Huang, L. Resnick, I. Shlimak, K. Sun, W. Xu, Scr. Mater. 61 (2009) 970–973.
[16] J. Grun, C.K. Manka, C.A. Hoffman, J.R. Meyer, O.J. Glembocki, R. Kaplan, S.B. Qadri, E.F. Skelton, D. Donnelly, B. Covington, Phys. Rev. Lett. 78 (1997) 1584–1587.
[17] K. Kirihara, Y. Shimizu, Y. Yamada, F. Esaka, T. Sasaki, N. Koshizaki, H. Yamamoto, S. Shamoto, K. Kimura, Appl. Phys. Lett. 97 (2010) 212105.
[18] I.H. Lee, A.Y. Polyakov, N.B. Smirnov, A.V. Govorkov, E. A. Kozhukhova, E.B. Yakimov, N.G. Kolin, V.M. Boiko, A. V. Korulin, S.J. Pearton, Appl. Phys. Lett. 98 (2011) 212107.
[19] X.L. Wu, T. Gao, G.G. Siu, S. Tong, X.M. Bao, Appl. Phys. Lett. 74 (1999) 2420–2422.
[20] Y. Maeda, Phys. Rev. B 51 (1995) 1658–1670.
[21] H.J. Zhu, Z.M. Jiang, A.M. Xu, M.C. Mao, D.Z. Hu, X.H. Liu, D. M. Huang, F. Lu, C.W. Hu, A.S. Kasuya, Prog. Nat. Sci. 8 (1998) 113–116.
[22] K.S. Min, K.V. Shcheglov, C.M. Yang, H.A. Atwater, M.L. Brongersma, A. Polman, Appl. Phys. Lett. 68 (1996) 2511–2513.
[23] J.K. Shen, X.L. Wu, R.K. Yuan, N. Tang, J.P. Zou, Y.F. Mei, C. Tan, X. M. Bao, G.G. Siu, Appl. Phys. Lett. 77 (2000) 3134–3136.
[24] M. Fujii, A. Mimura, S. Hayashi, Y. Yamamoto, K. Murakami, Phys. Rev. Lett. 89 (2002) 206805.
[25] A. Mimura, M. Fujii, S. Hayashi, D. Kovalev, F. Koch, Phys. Rev. B 62 (2000) 12625.
[26] M. Fujii, A. Mimura, S. Hayashi, K. Yamamoto, C. Urakawa, H. Ohta, J. Appl. Phys. 87 (2000) 1855–1857.
[27] K. Toshikiyo, M. Tokunaga, S. Takeoka, M. Fujii, S. Hayashi, K. Moriwaki, J. Appl. Phys. 90 (2001) 5147–5151.
[28] K. Toshikiyo, M. Tokunaga, S. Takeoka, M. Fujii, S. Hayashi, J. Appl. Phys. 89 (2001) 4917–4920.